

Binary semiconductor In_2Te_3 for the application of phase-change memory device

Hao Zhu · Kai Chen · Zhongyang Ge · Hanni Xu ·
Yi Su · Jiang Yin · Yidong Xia · Zhiguo Liu

Received: 21 October 2009 / Accepted: 8 March 2010 / Published online: 23 March 2010
© Springer Science+Business Media, LLC 2010

Abstract Nonvolatile phase-change memory devices with 500 nm contact hole based on In_2Te_3 were successfully fabricated by using focused ion beam, pulsed laser deposition, and dc magnetic sputtering techniques. In_2Te_3 films were characterized by using differential thermal analysis, X-ray diffraction, and UV-vis diffuse absorption spectroscopy, respectively. The devices can be switched between high and low resistance states repeatedly with the programmed voltage pulses. The reset operation (crystalline to amorphous) was done by the voltage pulse with a magnitude of 3.5 V and a duration of 30 ns, and the set operation (amorphous to crystalline) was done by the voltage pulse with a magnitude of 1.4 V and a duration of 100 ns. A dynamic resistance switching ratio (OFF/ON ratio) of 3.2×10^3 has been obtained.

Introduction

The rapid development of semiconductor technology and digital electronic devices has created huge demand for new nonvolatile memory, which should have high density, low power consumption, high speed, good endurance for repetitive reading and writing, and good compatibility with complementary metal-oxide-semiconductor (CMOS) chips

[1–4]. One of the promising candidates is the phase-change random access memory (PRAM) [5–8]. Materials, especially chalcogenide compounds that are stoichiometric, with reversible crystalline-amorphous-crystalline transformations exhibit states with quite distinct resistance. These resistance states can be switched by controlling the temperature or the electric field, which is the basis for PRAM [9]. Ovshinsky brought forward the proposition about PRAM in 1968 for the first time [10], but almost no progress had been achieved during the following 20 years. In recent decades, attention has been brought back to PRAM, as its advantages over charge storage memories have been comprehended and studied [11–13]. Now great efforts have been made to explore phase-change materials which are potentially suited for PRAM, and it has been revealed that there are relationships among stoichiometry, structure, physical properties, and suitability of PRAM [14, 15]. These researches on the essential properties for phase-change materials have provided people much easier and more efficient ways for the identifications of phase-change materials.

Until now, a few chalcogenide compounds have been investigated. Among these chalcogenide compounds, $\text{Ge}_2\text{Sb}_2\text{Te}_5$ (GST) has been widely used, especially in DVD and non-volatile memory devices due to its fast crystalline-amorphous-crystalline transformations [6, 7, 16]. The GST devices can be switched between ON (low resistance) state and OFF (high resistance) state by irradiating with special pulsed laser beams or heating with programmed voltages pulses. The ‘ON’ and ‘OFF’ states are identified by the difference in the electrical resistance that is read by applying a much lower dc voltage without disturbing the structure of films. The dynamic switching ratio of $R_{\text{OFF}}/R_{\text{ON}}$ should be sufficiently large for further nonvolatile PRAM applications. In this paper, we report a new phase-

H. Zhu · K. Chen · Z. Ge · J. Yin (✉)
National Laboratory of Solid State Microstructures
and Department of Physics, Nanjing University,
Nanjing 210093, People's Republic of China
e-mail: jyin@nju.edu.cn

H. Xu · Y. Su · Y. Xia · Z. Liu
National Laboratory of Solid State Microstructures
and Department of Materials Science and Engineering, Nanjing
University, Nanjing 210093, People's Republic of China

change material In_2Te_3 for PRAM with a simple composition, wide band-gap, and excellent electrical switching properties.

Experimental

In_2Te_3 films were deposited on Si (111) substrates by using the pulsed laser deposition (PLD) technique with a KrF excimer laser (COMPEx, Lambda physic, 248 nm in wavelength, 30 ns in pulse width). The In_2Te_3 bulk prepared from 99.99% pure elements by using levitation melting method was used as a target. The laser runs at 5 Hz with an average energy of 250 mJ. The whole experiment was performed in a vacuum chamber with a base pressure of 10^{-4} Pa. The films were deposited at room temperature for 15 min, and the thickness is about 500 nm, as checked by using α -step device. As learned from the differential thermal analysis (DTA) results that the crystallization temperature of $\alpha\text{-In}_2\text{Te}_3$ is about 463 °C, these amorphous films as-deposited were then in situ annealed at 460 °C in the vacuum chamber with a base pressure of 10^{-4} Pa for 20 min in order to make sure that the amorphous films get fully crystallized.

The In_2Te_3 films were characterized by energy dispersive X-ray spectroscopy (EDS), DTA, X-ray diffraction (XRD), and UV-vis diffuse absorption spectroscopy. A field-emission scanning electron microscope (LEO 1530VP) was used for the study of the morphology and composition of In_2Te_3 films. The DTA study was performed by using a NETZSCH STA 449C with a heating rate of 10 K/min. The XRD patterns were obtained using a Rigaku D/max 2500VL/PC X-ray diffractometer, with a power of 4 kW (40 kV, 100 mA) and a scanning speed of 2°/min. During the measurement of the UV-vis diffuse absorption spectra, the In_2Te_3 films were firstly deposited on quartz substrate by PLD technique with a thickness of about 500 nm, and then a Shimadzu UV-3600 UV-vis spectrophotometer was employed to obtain the absorption spectra. Here we choose the quartz substrate because the band gap of the quartz is much larger than that of In_2Te_3 films, which is helpful for the determination of band gaps of In_2Te_3 films.

In_2Te_3 phase-change memory devices included a layer of In_2Te_3 film sandwiched between a top and a bottom Pt electrode, similar with that described in [17]. The bottom Pt film was firstly deposited on a silicon wafer with dc magnetic sputtering method. Then the PECVD deposition of SiO_2 film with a thickness of 200 nm was performed on the substrate. By using the focused ion beam (FEI, strata FIB201) technique, a circular hole with a diameter of 500 nm was etched in the insulating SiO_2 film, exposing the bottom Pt film. A layer of In_2Te_3 film with a thickness

of 200–300 nm was deposited directly on the top of bottom electrode by using PLD technique, and then a 100-nm-thick top Pt electrode was deposited by using dc magnetic sputtering method.

The current–voltage ($I\text{-}V$) characteristics of the devices were measured by using a Keithley 2400 source-measure unit. In the SET and RESET operations of the devices, an Agilent 81104A Pulse-/Pattern Generator were employed to provide voltage pulses. All the measurements were performed at room temperature.

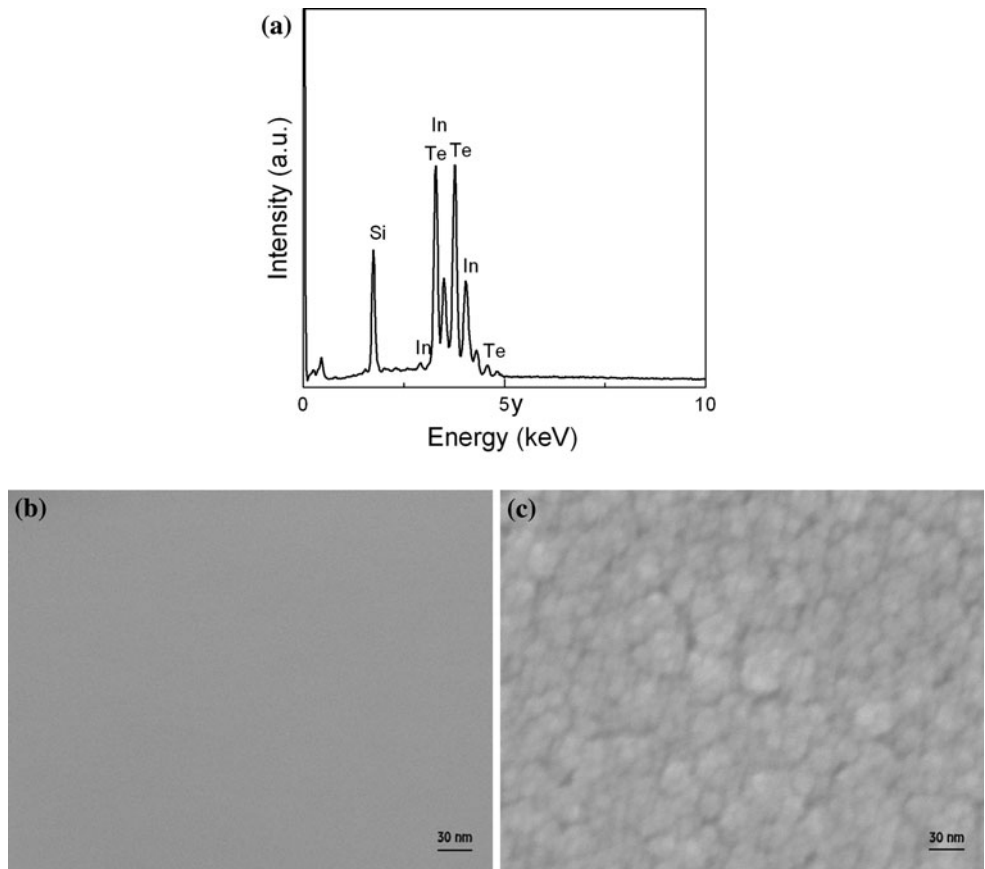
Results and discussion

Zaslavskii and Sergeeva [18] have discovered two kinds of structure for In_2Te_3 , as α - and $\beta\text{-In}_2\text{Te}_3$. In our study, we only focus on $\alpha\text{-In}_2\text{Te}_3$ crystalline phase, as the transformation temperature of β phase is much higher than that of α phase, and closer to the melting point, which can be determined by DTA. $\alpha\text{-In}_2\text{Te}_3$ has a face-centered cubic structure ($a = 18.5$ Å), that is preferable for high speed phase-change materials, since they enable fast crystallization due to the simple crystal structure.

Figure 1a is the energy dispersive X-ray spectroscopy (EDS) of the amorphous In_2Te_3 film, which was shown near the stoichiometric ratio as designed (the EDS results of crystalline In_2Te_3 films were similar to that of amorphous films, which were not shown here). Figure 1b, c is scanning electron microscopy images of as-deposited and annealed In_2Te_3 films, respectively. Crystal grains of about 30 nm size were precipitated by the annealing process.

Figure 2a shows the DTA result of the amorphous films deposited at room temperature. During heating up to 650 °C at a heating rate of 10 °C/min, two exothermic peaks appear at 463.3 and 629.6 °C, respectively. The former peak demonstrates the transition from the glass phase to the crystalline phase ($\alpha\text{-In}_2\text{Te}_3$), while the latter one shows the transformation from $\alpha\text{-In}_2\text{Te}_3$ to $\beta\text{-In}_2\text{Te}_3$. Zaslavskii and Sergeeva [18] have reported that the transition from α to β occurs at about 620 °C, which is in accordance with our data of 629.6 °C. Figure 2b shows XRD pattern of the In_2Te_3 bulk and the films as-deposited and annealed at 460 °C, respectively. The results demonstrate that after annealing, the amorphous In_2Te_3 film has transformed to the crystalline phase, and the XRD pattern of the crystalline film is still identical to that of the In_2Te_3 bulk. The UV-vis spectrometer measurements of amorphous and crystalline (after annealing at 460 °C) In_2Te_3 films were also performed to determine the optical gap, as shown in Fig. 2c. We obtain the absorption spectra of both amorphous and crystalline films by the UV-vis measurements. We calculate the band gaps of both films with the following equation as described in [19, 20]:

Fig. 1 **a** EDS spectrum of the amorphous In_2Te_3 film, with 40.07 at.% In and 59.93 at.% Te. Si peaks originates from the substrate; **b** SEM image of In_2Te_3 film as-deposited; **c** SEM image of annealed In_2Te_3 films



$$\alpha h\nu = A(h\nu - E_g)^n/2$$

where α , ν , E_g , A , and n are the absorption coefficient, incident light frequency, band gap, constant, and an integer, respectively. Here the value of n as determined for both amorphous and crystalline In_2Te_3 is 1, indicating that the optical transition shown in figure is directly allowed. Since In_2Te_3 is a direct band gap semiconductor, the optical gap can be deduced from the plot of $(\alpha h\nu)^2$ vs. photon energy by extrapolating straight line, as shown in the insets of Fig. 2c. The band gaps of the amorphous and crystalline In_2Te_3 films were determined as about 1.54 and 1.66 eV, respectively. So a 0.12 eV narrowing of the optical bandgap in the amorphous In_2Te_3 film as compared with the crystalline $\alpha\text{-In}_2\text{Te}_3$ films is formed, resulting from the band tailing effects in the extrema of the conduction and valence bands [21–23]. As a result, a large optical contrast is obtained between the amorphous and the crystalline films, enabling $\alpha\text{-In}_2\text{Te}_3$ as a PCM to be employed in optical data storage.

The typical switching behavior of our PRAM devices with $\alpha\text{-In}_2\text{Te}_3$ film by voltage sweeping is shown in Fig. 3. In_2Te_3 films were deposited at room temperature, so the initial state of the film used in the device is amorphous. During I-V measurement with a low applied voltage, only

a low current flows through the cell due to the high resistance of the amorphous In_2Te_3 film. However, the current of the device increased suddenly when the applied voltage was greater than a threshold value of 0.3 V. Over this threshold voltage, the amorphous In_2Te_3 film in the device undergoes a fast electronic transition (threshold switching [24, 25]) to a much lower resistance state. So a much larger current flows through the device, producing enough heat to crystallize the amorphous In_2Te_3 film. As a result, the amorphous In_2Te_3 film was switched to the crystalline state. The second sweep only shows ohmic behavior, because the crystallization transition of the material has been completed during the first sweep.

Figure 4a, b shows the reset and set operations with programmed voltage pulses. After the current–voltage measurement, the film used in the device was in the crystalline state (low resistance), with a resistance of about 10 Ω . By applying a sequence of voltage pulses with constant duration but varying magnitude, the device was reset to the amorphous state (high resistance, ‘OFF’ state) with a resistance of about $2 \times 10^4 \Omega$, as shown in Fig. 4a. The threshold magnitude of the reset voltage pulse is 3.5 V with a duration of 30 ns (with a 3 ns sharp fall-down edge). As described earlier, the reset voltage pulse heated the device to a temperature above the melting point, and the

Fig. 2 **a** DTA graph of the amorphous In_2Te_3 films, and the heating rate is 10 K/min; **b** (i) XRD pattern of In_2Te_3 bulk, (ii) XRD pattern of In_2Te_3 films annealed at 460 °C, (iii) XRD pattern of In_2Te_3 films grown at room temperature; **c** UV-vis diffuse absorption spectra of the amorphous and crystalline In_2Te_3 films. Insets: Plots of $(\alpha h\nu)^2$ vs. photon energy for crystalline and amorphous films

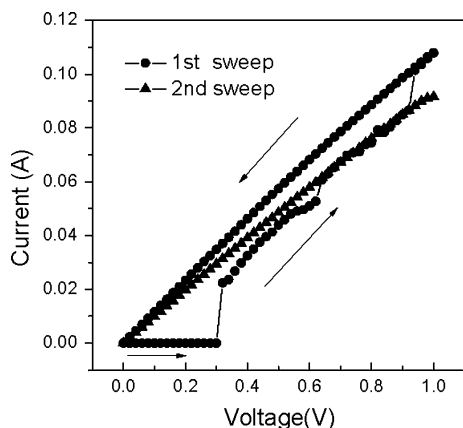
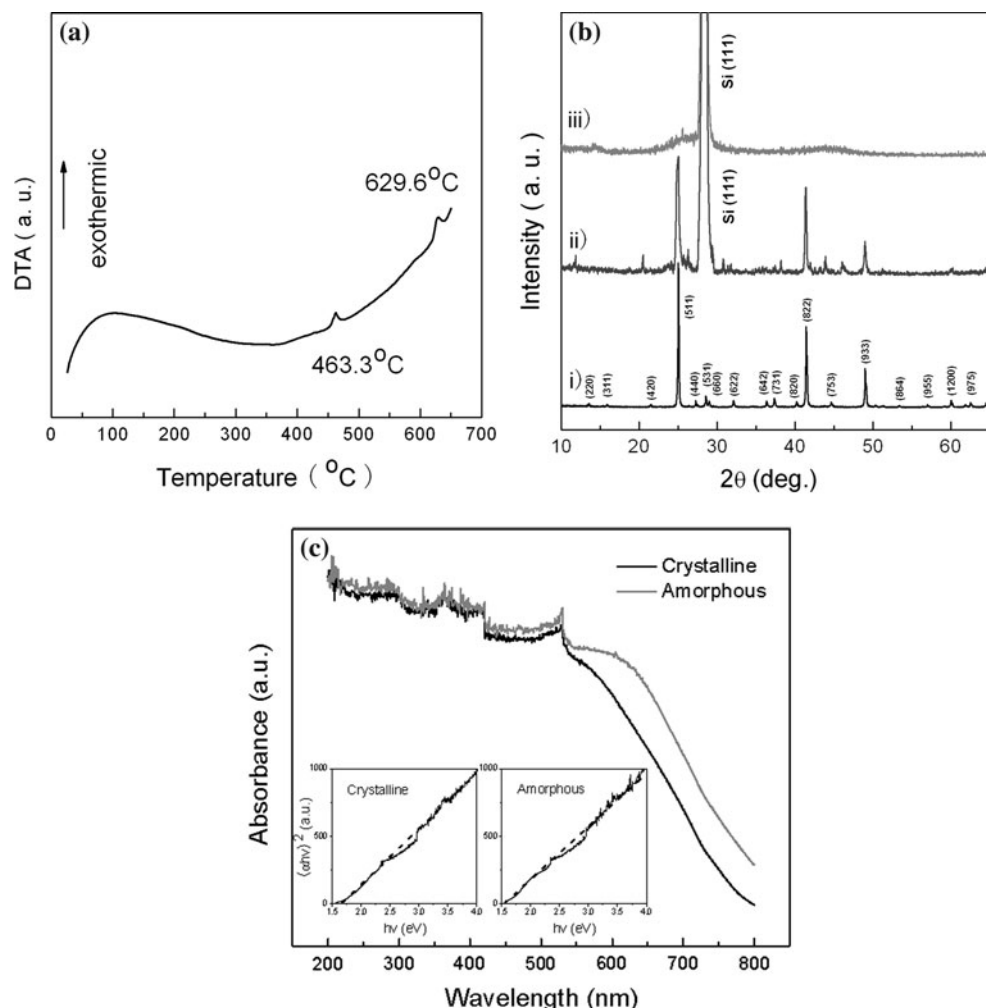


Fig. 3 Typical current–voltage curve of phase-change memory device with an initial amorphous In_2Te_3 film

following rapid quenching (the 3 ns fall-down edge) leads to the transformation of the crystalline In_2Te_3 film to the amorphous state. It should be also noted that an intermediate state with a resistive level of about 100Ω was reached when the magnitude of the reset voltage pulse was

2–3 V, which could be possibly associated with the formation of the partially amorphousized In_2Te_3 film. Then, the device in high resistance state was subjected to a series of voltage pulses with a lower magnitude but a longer duration (the pulse width was set to 100 ns). The device remains a constant resistance of about $2 \times 10^4 \Omega$ till 1.0 V, and then the resistance of the device falls sharply until it was set to the crystalline state ('ON' state) with a low resistance of about 10Ω at 1.4 V, as shown in Fig. 4b. The set voltage pulse with a long duration heated the device upon the crystalline temperature while below the melting point, which could be considered as an annealing process, and hence rendered the transformation of the amorphous film to crystalline state. All the above readings (measurements) on the resistance were accomplished by using a dc voltage of 0.1 V.

Figure 5 shows the repeated resistive switching operations of In_2Te_3 phase-change memory device. The switching operation was done by alternating the magnitude and the duration of the voltage pulses. In our study, the device was set to the low resistance state by using a 1.4 V

Fig. 4 Switching behavior of In_2Te_3 phase-change memory device: **a** reset at 3.5 V 30 ns, **b** set at 1.4 V 100 ns

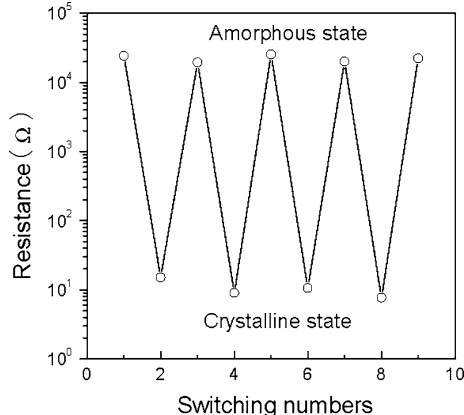
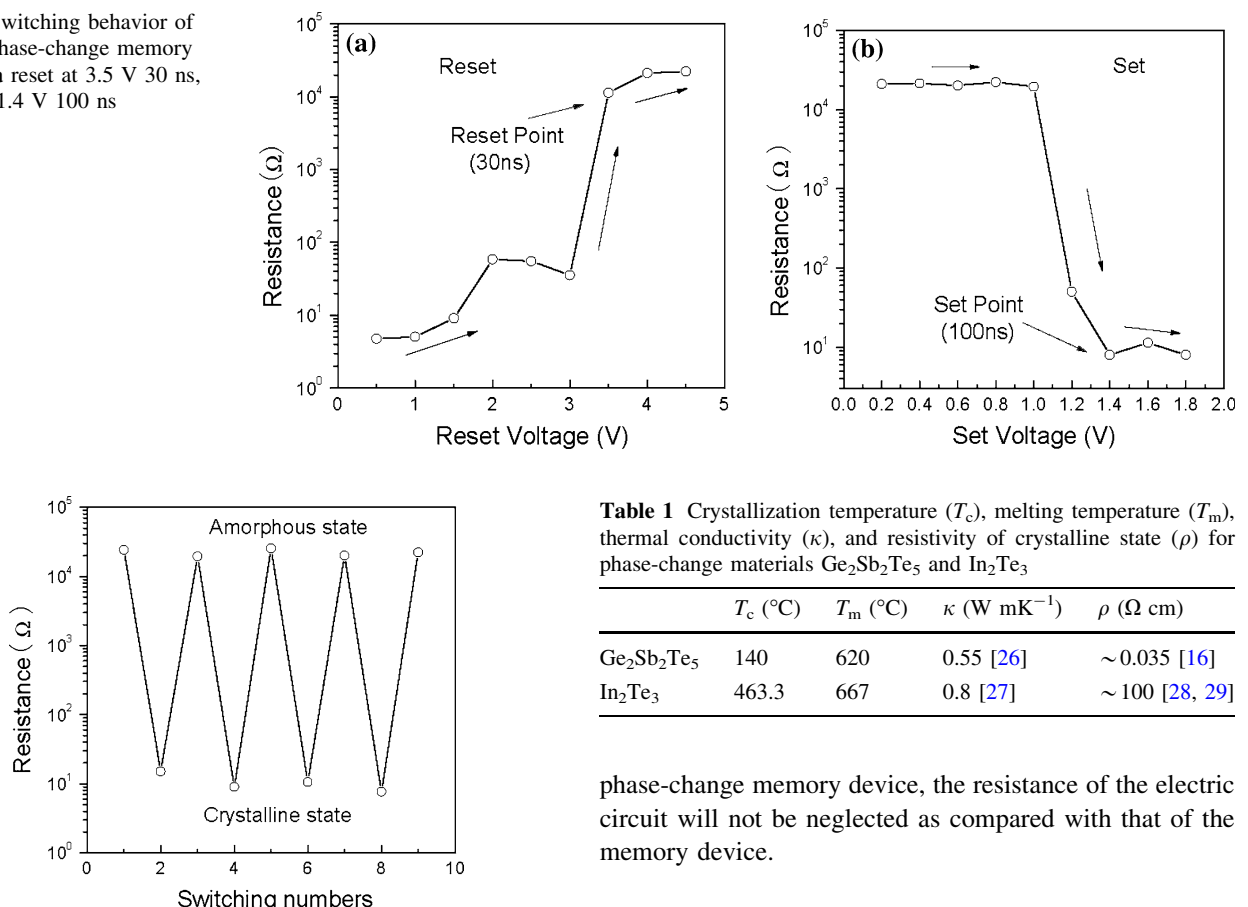


Fig. 5 Repeated switching of In_2Te_3 phase-change memory device. Device was switched between amorphous and crystalline states by applying respective voltage pulses

pulse with pulse duration of 100 ns, and reset to the high resistance state by using a voltage pulse with a magnitude of 3.5 V pulse and a duration of 30 ns. The device shows a high dynamic switching ratio of 3.2×10^3 , although the trace variations of the resistance in the low and the high resistance states during the measurement were observed. Considering the energy requirement during the memory switching, the power needed for Reset operation given by V^2/R is 1225 mW at 3.5 V. The corresponding energy input is 36.8 nJ for the 30 ns pulse. The power required for the set operation is 196 mW with an energy input of 19.6 nJ for the 100 ns pulse. For comparison, some physical properties of In_2Te_3 and GST were compared and listed in Table 1. Particularly, the much higher resistivity of the crystalline In_2Te_3 film enables the memory cell to possess a higher resistance of the crystalline state as compared with that of $\text{Ge}_2\text{Sb}_2\text{Te}_5$ phase-change memory cell. This behavior is not only important for minimizing the power consumption of the memory cell (reducing the reset current), but also for the design of the driving electric circuit of PRAMs, because with the scaling down of the size of

Table 1 Crystallization temperature (T_c), melting temperature (T_m), thermal conductivity (κ), and resistivity of crystalline state (ρ) for phase-change materials $\text{Ge}_2\text{Sb}_2\text{Te}_5$ and In_2Te_3

	T_c (°C)	T_m (°C)	κ (W mK $^{-1}$)	ρ (Ω cm)
$\text{Ge}_2\text{Sb}_2\text{Te}_5$	140	620	0.55 [26]	~ 0.035 [16]
In_2Te_3	463.3	667	0.8 [27]	~ 100 [28, 29]

phase-change memory device, the resistance of the electric circuit will not be neglected as compared with that of the memory device.

Conclusion

The prototypical phase-change memory devices with In_2Te_3 as a novel phase-change material have been fabricated by using FIB and PLD techniques. The devices show sufficient contrast in their resistances between the high resistance state ($2 \times 10^4 \Omega$) and the low resistance state (10Ω), which can be set or reset by using a voltage pulse with different magnitude and duration. A high dynamic switching ratio of 3.2×10^3 has been obtained. Phase-change material In_2Te_3 with a simple composition, wider band gap, fast electrical switching speed, and a high dynamic resistance switching ratio is of attractive potential to be a promising candidate for the application in PRAM in the future.

Acknowledgements This work was supported financially by the state key program for basic research of China under the Grant No. of 2007CB935401 and 2006CB921803.

References

1. Wuttig M, Steimer C (2007) Appl Phys A Mater Sci Process 97:411
2. Hudgens S, Johnson B (2004) MRS Bull 11:829

3. Feinleib J, Neufville J, Moss SC, Ovshinsky SR (1971) *Appl Phys Lett* 18:254
4. Liu B, Zhang T, Xia JL, Song ZT, Feng SL, Chen B (2004) *Semicond Sci Technol* 19:L61
5. Yamada N, Ohno E, Akahira N, Nishiuchi K, Nagata K, Takao M (1987) *Jpn J Appl Phys* 26:61
6. Wuttig M, Yamada N (2007) *Nature Mater* 6:824
7. Yamada N, Ohno E, Nishiuchi K, Akahira N (1991) *J Appl Phys* 69:2849
8. Pirovano A, Lacaia AL, Benvenuti A, Pellizzer S, Bez R (2004) *IEEE Trans Electron Devices* 51:452
9. Kolobov AV, Fons P, Frenkel AI, Ankudinov AL, Tominaga J, Uruga T (2004) *Nat Mater* 3:703
10. Ovshinsky SR (1968) *Phys Rev Lett* 21:1453
11. Kang D, Ahn D, Kwon M, Kwon H, Kim K, Lee K, Cheong B (2004) *Jpn J Appl Phys* 43:5243
12. Lankhorst M, Ketelaars B, Wolters R (2005) *Nat Mater* 4:347
13. Wuttig M (2005) *Nat Mater* 4:265
14. Lencer D, Salina M, Grabowski B, Hickel T, Neugebauer J, Wuttig M (2008) *Nat Mater* 7:972
15. Frumar M, Frumarova B, Wagner T, Hrdlicka M (2007) *J Mater Sci Mater Electron* 18:169
16. Lacaia AL, Wouters DJ (2008) *Phys Stat Sol (a)* 205:2281
17. Guo HX, Yang B, Chen L, Xia YD, Yin KB, Liu ZG, Yin J (2007) *Appl Phys Lett* 91:243513
18. Zaslavskii AI, Sergeeva VM (1961) *Sov Phys Sol State* 2:2556
19. Yin J, Zou Z, Ye J (2002) *J Mater Res Rapid Commun* 17:2201
20. Butler MA (1977) *J Appl Phys* 48:1914
21. Leyral P, Bois D, Pinard P (2006) *Phys Stat Sol (b)* 73:187
22. Mieghem V (1992) *Rev Mod Phys* 64:755
23. Zhao GY, Ishikawa H, Jiang H, Egawa T, Jimbo T, Umeno M (1999) *Jpn J Appl Phys* 38:993
24. Kastner M, Adler D, Fritzsche H (1976) *Phys Rev Lett* 37:1504
25. Redaelli A, Pirovano A, Benvenuti A, Lacaia AL (2008) *J Appl Phys* 103:111101
26. Fallica R, Battaglia JL, Cocco S, Monguzzi C, Teren A, Wiemer C, Varesi E, Cecchini R, Gotti A, Fanciulli M (2009) *J Chem Eng Data* 54:1698
27. Kuroasaki K, Matsumoto H, Charoenphakdee A, Yamanaka S, Ishimaru M, Hirotsu Y (2008) *Appl Phys Lett* 93:012101
28. Sayama S, Ishimaru M, Charoenphakdee A, Matsumoto H, Kuroasaki K (2009) *J Electron Mater* 38:1392
29. Desai RR, Lakshminarayana D, Patel PB, Panchal CJ (2006) *J Mater Sci* 41:2019. doi:[10.1007/s10853-006-4502-x](https://doi.org/10.1007/s10853-006-4502-x)